Two Ising Models Coupled to 2–Dimensional Gravity

Mark Bowick, Marco Falcioni,
Geoffrey Harris and Enzo Marinari(*)

Dept. of Physics and NPAC,
Syracuse University,
Syracuse, NY 13244-1130, USA
bowick falcioni gharris @npac.syr.edu
marinari@roma1.infn.it

(*): and Dipartimento di Fisica and INFN,
Università di Roma *Tor Vergata*
Viale della Ricerca Scientifica, 00173 Roma, Italy

February 4, 1994

Abstract

To investigate the properties of $c = 1$ matter coupled to 2d–gravity we have performed large-scale simulations of two copies of the Ising Model on a dynamical lattice. We measure spin susceptibility and percolation critical exponents using finite-size scaling. We show explicitly how logarithmic corrections are needed for a proper comparison with theoretical exponents. We also exhibit correlations, mediated by gravity, between the energy and magnetic properties of the two Ising species. The prospects for extending this work beyond $c = 1$ are addressed.

SU-HEP-93-4241-556
SCCS 540
hep-th/yymmnnn

1 Introduction

There is at present considerable analytic understanding of how conformal matter with central charge (c) less than or equal to one couples to two-dimensional gravity [1]. These $c \leq 1$ models are relevant both as non-critical string theories and as novel statistical mechanical systems describing matter on a dynamical substrate lattice. The relation of these models to quantum Liouville theory [2] allows one to compute the shift in the scaling dimension of physical operators due to the coupling to 2d-gravity. This shift is determined solely by the scaling dimension of the operator in the absence of gravity (i.e on a fixed lattice) and the central charge of the theory. Given the dressed scaling dimensions one can compute critical exponents of thermodynamic observables related to correlation functions. Through the mapping of these systems onto matrix models it is even possible to incorporate topology change by performing the entire sum over topologies in the so-called double-scaling limit.

This beautiful state of affairs falls apart for central charge exceeding one[1]. In this case the methods of Liouville theory appear to fail - in particular they predict complex critical exponents. The vanishing of the mass of the dressed identity operator (the tachyon) at $c = 1$ suggests the onset of an instability in the worldsheet geometry. Based on this, it is widely believed that $c > 1$ no longer describes a continuum theory of surfaces [4]. Since no models have been solved in this regime, it would be valuable to apply numerical techniques to see if $c > 1$ models appear to be qualitatively different than those with $c < 1$.

A simple class of models to test our understanding of these issues is provided by multiple copies of the Ising model on a dynamical lattice. Each Ising model has $c = \frac{1}{2}$. A model with n individual copies then has $c = n/2$. For a single Ising model ($n = 1$) on a dynamical lattice the critical exponents may be computed analytically via a mapping of the model onto a particular 2-matrix model (with one matrix representing spin up and the other spin down) [5, 6]. The model has a third order rather than a second order phase transition. Without the coupling to gravity the partition function of the n-Ising model would simply be the n–th power of the single Ising model partition function, since the spins of different copies are independent. The interaction with gravity, however, induces an effective interaction between spins of different species (copies). Spins of different species effectively interact through the dynamical lattice. Brézin and Hikami [7, 8, 9] have studied an equivalent 2^n-matrix model realization of this system in perturbation theory in the cosmological constant, without any apparent anomaly setting in at $c = 1$. Similarly Monte-Carlo studies of multiple–Ising and multiple–Potts models on dynamically-triangulated random surfaces (DTRS) do not uncover dramatic changes as c passes through one [10, 11, 12].

On the numerical side it is important that we understand the transition case $c = 1$ before plunging into the regime $c > 1$. This is the motivation for the work presented in this paper on large-scale DTRS simulations of the $n = 1$ and $n = 2$ Ising model coupled to 2d-gravity. In the $n = 2$ case the formalism of KPZ allows a computation of the relevant critical exponents, which we can consequently compare to the numerical results extracted from finite-size scaling and direct fits. The exact solution of the single-Ising model also provides a direct check that the discrete DTRS algorithm is reproducing continuum behavior for the lattice sizes simulated and that the numerical analysis methods employed are adequate. The $n = 2$ ($c = 1$) case is considerably more complicated than the $n = 1$ case because of logarithmic violations of scaling. Here the extensive work on $c = 1$ matrix models provides an essential clue [13]. It allows us to identify the appropriate scaling variable that replaces the cosmological constant. With this in hand we are able to compare the results of our large-scale DTRS Monte-Carlo simulations with the predictions of KPZ.

[1] More precisely when the quantity $c - 24\Delta > 1$, where Δ is the conformal weight of the lowest-weight state in the theory [3].

Similar issues are also addressed in a companion paper [14] in which percolation coupled to gravity with $c = 0, 1/2, 1$ and $c > 1$ matter is examined in much detail. The nature of finite size effects in simulations of two dimensional gravity plays a central role in that paper, as it does here. We shall show how the percolation results for Gaussian matter in [14] are consistent with those obtained in the two species Ising model discussed here.

The outline of the rest of the paper is as follows. In section 2 we give a theoretical discussion of $c = 1$ conformal matter coupled to 2d-gravity, with a derivation of the critical exponents we will be comparing with our numerical simulations and a discussion of logarithmic violations of scaling. In section 3 we present our numerical methods and results including a comparison with theoretical expectations. Finally, in section 4, we conclude with a discussion of the origin of logarithmic corrections to scaling and the prospects for extending this work to the regime $c > 1$ that this implies.

2 Theoretical Predictions

We shall consider a model in which Ising spins are attached to the vertices of triangulations. The triangulations are characterized by their adjacency matrix C_{ij} which equals 1 if i and j are neighbors and vanishes otherwise. C_{ij} is the discrete analogue of the worldsheet metric g_{ij}. We shall restrict ourselves to the set of triangulations with N vertices $\mathcal{T}_N$ containing only loops of length 3 or greater and vertices of coordination number of at least 3. We simulate a theory determined by the partition function

$$Z_N = \sum_{T \in \mathcal{T}_N} \sum_{\sigma_i = \pm 1} \exp(-\beta \sum_{\alpha=1}^{n_s} \sum_{i,j=1}^{N} C_{ij}(T) \sigma_i^\alpha \sigma_j^\alpha); \qquad (1)$$

α labels the spin species. In this paper, we address the cases $n_s = 1$ and 2. Most of the relevant theoretical calculations are performed in the grand-canonical ensemble, with the partition function

$$Z(\mu) = \sum_{N=1}^{\infty} Z_N \exp(-\mu N) \qquad (2)$$

dependent on μ, the cosmological constant.

Our primary observable will be the spin–susceptibility, which we express as

the integrated spin–spin correlation function

$$\chi_N = \frac{1}{n_s\ N}\ \langle \sum_{\alpha=1}^{n_s} \sum_{i,j} \sigma_i^\alpha \sigma_j^\alpha \rangle. \tag{3}$$

The integrated spin–spin correlation function in the grand–canonical ensemble then satisfies

$$\langle \sum_{\alpha=1}^{n_s} \sum_{i,j} \sigma_i^\alpha \sigma_j^\alpha \rangle(\mu) Z(\mu) = \sum_{N=1}^{\infty} n_s N \chi_N Z_N \exp(-\mu N). \tag{4}$$

Using standard arguments [15] one can determine how the scaling behavior of the integrated spin–spin correlation function changes under coupling to gravity. In flat space, the spin–spin correlation functions scales as

$$\langle \sigma_i^\alpha \sigma_j^\alpha \rangle \sim |\vec{r}_i - \vec{r}_j|^{-2(\Delta_\sigma^o + \bar{\Delta}_\sigma^o)}. \tag{5}$$

The weight $\Delta_\sigma^o = \bar{\Delta}_\sigma^o = 1/16$ is dressed by gravity in a theory of central charge c according to the KPZ formula [2]

$$(\Delta_\sigma - \Delta_\sigma^o) = \left(1 + \frac{1}{12}\left(\sqrt{1-c} - \sqrt{25-c}\ \right)\sqrt{1-c}\right)\Delta_\sigma(1-\Delta_\sigma). \tag{6}$$

This dressed weight determines the scaling of the integrated spin–spin correlation function with μ on surfaces of genus h:

$$\langle \sum_{\alpha} \sum_{i,j} \sigma_i^\alpha \sigma_j^\alpha \rangle(\mu) Z(\mu) \sim (\mu - \mu_c)^{2(-1+\Delta_\sigma)+(2-\gamma_s)(1-h)} \tag{7}$$

(the -1 before the dressed weight accounts for the integrations of i and j over the surface) with

$$\gamma_s = \frac{1}{12}\left(c - 1 - \sqrt{(25-c)(1-c)}\right). \tag{8}$$

The above relations (4) and

$$Z_N \sim N^{-1+(\gamma_s-2)(1-h)} \tag{9}$$

yield the finite-size scaling relation

$$\chi_N \sim N^{\gamma/\nu d_H}, \tag{10}$$

with

$$\gamma/\nu d_H = 1 - 2\Delta_\sigma. \tag{11}$$

This is the scaling law that we shall verify numerically. The susceptibility scales as $\chi \sim (\beta - \beta_c)^{-\gamma}$, the correlation length (governed by the decay of the spin–spin correlation function) obeys $\xi \sim (\beta - \beta_c)^{-\nu}$ and d_H is the intrinsic Hausdorff dimension of the random surface being considered.

Assuming the standard scaling hyperscaling relation $\alpha = 2 - \nu d_H$, we can also predict the value of γ. The specific heat scales as $N^{\alpha/\nu d_H}$. Then by applying the reasoning used to arrive at (11) to the two-point function of the energy operator ε, one finds $\alpha/\nu d_H$ equals $1 - 2\Delta_\varepsilon$, where Δ_ε is the dressed weight of the energy operator. It then follows that

$$\gamma = \frac{(1-2\Delta_\sigma)}{(1-\Delta_\varepsilon)}. \tag{12}$$

One obtains Δ_ε through the KPZ formula (6), substituting the bare energy weight $\Delta_\varepsilon^o = 1/2$ for Δ_σ^o.

We shall also measure scaling properties of the Fortuin-Kasteleyn (FK) clusters [16] which we construct to update the spin degrees of freedom. The FK clusters appear in the reformulation of the Ising model as a correlated spin–bond percolation model with partition function [17]

$$Z = \sum_{\sigma_i = \pm 1} \sum_{colorings} p^b (1-p)^{N_b - b}. \tag{13}$$

Colorings consist of a set of 'black' bonds drawn between adjacent points with identical spin values; each black bond is drawn with probability $p = 1 - \exp(-2\beta)$. In (13) b bonds out of a possible N_b bonds of the lattice are colored black. FK clusters comprise sets of sites linked together by black bonds. Therefore each cluster is assigned a single spin value. In the multi-generation case, we build a set of colored bonds and FK clusters separately for each species of spin. One can show that the spin–spin correlation function of the spins $\langle \sigma_i^\alpha \sigma_j^\alpha \rangle$ equals the pair-connectedness function $\langle \delta_{\mathcal{C}_i^\alpha, \mathcal{C}_j^\alpha} \rangle$ of the corresponding FK clusters; δ is 1 when i and j lie in the same cluster $\mathcal{C}^\alpha$ and 0 otherwise [18]. From this, it follows that the spin–susceptibility equals the mean cluster size $\mathcal{S} = \langle s^2 \rangle / \langle s \rangle$, in which averages are taken over the distribution $n(s)$, the mean number of clusters per configuration containing s sites. We thus shall determine the scaling of the mean-cluster size and in addition, the fractal dimension d_f of the largest cluster. The average maximal size cluster $\mathcal{M}$ of each configuration scales as

$$\mathcal{M} \sim N^{\frac{d_f}{d_H}}. \tag{14}$$

Standard scaling arguments [19] relate $\gamma/\nu d_H = 2d_f/d_H - 1$. One can derive this, for instance, by considering the asymptotic form of $n(s) \sim N s^{-\tau}$. The

standard hyperscaling relation $\nu d_H = 2 - \alpha$ is then needed. The singularity of the cluster number density, the zeroth moment of $n(s)$, as a function of $p - p_c$, is given by the exponent $(2 - \alpha)$. Similarly the second moment of $n(s)$ scales as $(p - p_c)^{-\gamma}$. Thus the usual scaling assumptions imply $\gamma/\nu d_H = (\tau - 3)/(1 - \tau)$. $\mathcal{M}$ asymptotically obeys

$$N \int_{\mathcal{M}}^{N} s^{-\tau} \sim 1 \tag{15}$$

(that is, the mean number of clusters per configuration of size greater than $\mathcal{M}$ is of order unity) and hence $d_f/d_H = 1/(\tau - 1)$. Eliminating τ then gives the above relation between d_f/d_H and $\gamma/\nu d_H$.

We can also obtain additional information about the critical geometry of these theories by examining the properties of pure percolation clusters. Consider the bond-percolation model

$$Z = \sum_{colorings} p^b (1-p)^{N_b - b} q^{N_c}, \tag{16}$$

which for $q = 2$ is yet another formulation of the Ising partition function and more generally is the partition function of the q-state Potts model. The pair-connectedness function then exhibits the scaling behavior at criticality of (5) with weights [20]

$$\Delta^o_{\sigma,q} = \bar{\Delta}^o_{\sigma,q} = \frac{(1-y^2)}{8(2-y)}; \quad \cos(\frac{\pi y}{2}) = \frac{1}{2}\sqrt{q}. \tag{17}$$

The $q \to 1$ limit corresponds to pure percolation, which has no dynamics (and vanishing central charge) and thus does not induce any back-reaction when it is coupled to a theory of gravity and matter of central charge c. $\Delta^o_{\sigma,q=1} = 5/96$; the dressed scaling of this weight is again governed by the KPZ formula (6). With this new dressed weight, we can then predict the scaling behavior of the mean (and maximal) cluster sizes $\mathcal{S}_{N,q=1}$ (and $\mathcal{M}_{N,q=1}$) using (10) with $\mathcal{S}$ substituted for χ.

In our simulations, we shall consider site percolation, in which sites (rather than bonds) are colored black with probability p and clusters are built by connecting adjacent colored sites. It is well known that bond and site percolation are in the same universality class, so that the scaling predictions described above should still hold in the case of pure site percolation. It is advantageous to consider site percolation because the critical value of p, p_c, is constrained to equal $1/2$ for site-percolation on triangulations [21][2].

[2] There are some possible exceptions to this constraint, which definitely do not apply in the cases we shall consider here. This issue is discussed extensively in [14].

2.1 $c = 1$

The scaling relations become more complicated for $c = 1$. Analytic solutions of the $c = 1$ matrix models (and a careful analysis of Liouville theory) show that correlation functions no longer scale simply as powers of the cosmological constant μ. Instead, the appropriate scaling variable is η which satisfies [3]

$$\mu = -\eta \ln(\eta) + c_1 \eta + \cdots \tag{18}$$

in the limit of small η; c_1 is a constant that we do not specify and shall not assume to be universal. This scaling relation has been derived for the Gaussian theory (of finite and infinite radius) coupled to gravity. The product of Ising models lies on the Gaussian $c = 1$ orbifold line [22]; coupled to gravity, it is not equivalent to the solved matrix models. We shall assume that the asymptotic logarithmic scaling violation is characteristic of $c = 1$ and thus holds in the two-species case. Then we conjecture that the scaling relation (7) should be modified so that [4]

$$\langle \sum_{i,j} \sigma^\alpha_i \sigma^\alpha_j \rangle(\mu) Z(\mu) \sim \eta(\mu)^{2(-1+\Delta_\sigma)+(2-\gamma_s)(1-h)}. \tag{19}$$

In the case of pure percolation, the pair-connectedness function should be substituted for the spin–spin correlation function, and the dressed Ising weight $\Delta_\sigma = 1/4$ should be replaced by $\Delta_{\sigma,q=1} = \sqrt{5/96}$. In the following formulae, χ and the mean cluster size $\mathcal{S}$ are interchangeable.

Our simulations will be done on worldsheets of toroidal topology ($h = 1$) for which $Z(\mu) \sim \ln(\eta)$ for $c = 1$ (for those models that have been solved analytically, so again we are making an assumption about universality). To extract the asymptotic scaling behavior of χ_N, we invert the relation between η and μ order by order in $1/\ln\mu$ and $\ln(-\ln(\mu))/\ln(\mu)$ to obtain

$$\eta = -\frac{\mu}{\ln\mu}\left(1 + \frac{\ln(-\ln\mu)}{\ln\mu} + \left(\frac{\ln(-\ln\mu)}{\ln\mu}\right)^2 - \frac{\ln(-\ln\mu)}{(\ln\mu)^2} + \cdots\right). \tag{20}$$

We then expand the inverse Laplace transform of (19) to obtain

$$N\chi_N Z_N \sim \frac{1}{N(N\ln N)^\omega}\left(1 - \frac{\ln\ln N}{\ln N} + \left(\frac{\ln\ln N}{\ln N}\right)^2 - \frac{\ln\ln N}{(\ln N)^2} + \cdots\right)^\omega \times \left(1 + \frac{\omega\Psi(-\omega)}{\ln N} - \omega\Psi(-\omega)\frac{\ln\ln N}{(\ln N)^2} + \cdots\right); \tag{21}$$

[3] Without loss of generality, we set $\mu_c = 0$.

[4] The essential role of logarithmic corrections in interpreting numerical measurements of γ_s at $c = 1$ has been previously discussed in reference [23].

$\omega = 2(-1+\Delta_\sigma) = -\gamma/\nu d_H - 1$ (or $\omega = 2(-1+\Delta_{\sigma,q=1})$ for pure site percolation) and Ψ is the digamma function. The scaling behavior of NZ_N is obtained by inverse Laplace transforming $\partial Z(\eta(\mu))/\partial\mu$:

$$Z_N \sim \frac{1}{N}\left(1 + \frac{1}{\ln N} - \frac{\ln\ln N}{(\ln N)^2} + \cdots\right). \tag{22}$$

In addition to the higher order terms that we have dropped from the inversion, there are additional corrections to the above formulae. The correction that depends on c_1 in (18), which we neglect, should lead to contributions to (21) and (22) that are competitive with the smallest corrections that we have included above. In addition, there should be the usual corrections to the scaling (19), but these will be suppressed by powers of $1/N$ and are negligible for moderately large N.

The difference in the theoretically predicted scaling behavior of percolation clusters at $c = 1$, compared to $c = 1/2$, illustrates the sensitivity of the worldsheet geometry to the presence of the Ising spins. This should induce an effective coupling between species, which we should be able to detect through correlations between different species' observables. To look for this coupling, we shall measure

$$e_{\alpha\beta} = \frac{1}{3N}\left(\langle E^\alpha E^\beta\rangle - \langle E^\alpha\rangle\langle E^\beta\rangle\right) \tag{23}$$

and

$$m_{\alpha\beta} = \frac{1}{N}\left(\langle|M^\alpha||M^\beta|\rangle - \langle|M^\alpha|\rangle\langle|M^\beta|\rangle\right) \tag{24}$$

with $E^\alpha = \sum_{ij} C_{ij}(T)\sigma_i^\alpha\sigma_j^\alpha$ and $|M^\alpha| = \sum_i |\sigma_i^\alpha|$. A nonzero effective coupling between species should then be manifest through the quantities $e^* = 2e_{12}/\mathrm{tr}\ e$ and $m^* = 2m_{12}/\mathrm{tr}\ m$, which vanish when E^α ($|M^\alpha|$) are uncorrelated and are 1 or -1 when they are respectively perfectly correlated or anti-correlated.

3 Numerical Simulations and Results

The partition function (1) is evaluated numerically by a Monte Carlo simulation. The sum over triangulations is implemented via the standard DTRS algorithm [24]. This updates the connectivity matrix C_{ij} by flips on randomly chosen pairs of triangles sharing a common link. The Ising spins are updated using the Swendsen-Wang algorithm [25]; one builds FK clusters over the entire lattice and then assigns a randomly chosen value to the spin associated with each cluster.

Runs were performed on lattices of toroidal topology of size $N = 2048, 4096, 8192$ and 16384. Each sweep consisted of $3N$ flips of randomly chosen

links followed by a Swendsen-Wang update of the spins. To perform the percolation measurements the sites on the lattice were then randomly colored and percolation clusters constructed. We used the jacknife technique to estimate our errors. We measured auto-correlation functions and computed integrated auto-correlation times, using standard techniques [17]. The magnetization, susceptibility and cluster sizes exhibited considerable critical slowing down [5]. It was necessary therefore to sample quite a large number of lattices - for each data point between 15,000 and 30,000 independent lattices, requiring from 30,000 to 900,000 sweeps. The total CPU-time used was approximately equivalent to six months on an HP-9000 (720) workstation. We histogrammed our data [27]. For cluster data on the larger lattices, however, histogramming was not reliable, given our statistics. The cluster data exhibited extremely large fluctuations from one measurement to the next; presumably this was the source of the poor performance of histogramming.

To extract critical exponents using finite-size scaling we must first determine the critical point. We estimated the value of β_c by locating the peak in the lattice susceptibility $\beta/N(\langle M^2\rangle - \langle|M|\rangle^2)$, where M is the magnetization averaged over species [6]. We first present our results for a single species. Figure 1 reveals that this quantity peaks at a value of $\beta_c = .2185(20)$. We also plotted Binder's cumulants [28] $U_M = 1 - \langle M^4\rangle/(3\langle M^2\rangle^2)$ as a function of β for different lattice sizes. From the position of the intersections of these cumulants, we estimate $\beta_c = .2180(7)$. The critical temperature for Ising spins on lattices dual to our triangulations was computed analytically in [29], so by the Ising duality relation, it follows that $\beta_c = (1/2)\ln(131/85) \sim .216273$. Our numerical estimate of the critical value of β is therefore somewhat high.

One could also envision locating the critical temperature by looking for a minimum of the mean pure percolation cluster size as a function of β. The growth in the mean cluster size is determined by the exponent $(\gamma/\nu d_H)_{q=1}$, which decreases with c. We would therefore expect that percolation clusters for a given lattice size will become smaller as c increases or likewise as β is tuned to bring the Ising spins to criticality. In Fig. 3 we do indeed observe a dip in the mean cluster size around the estimated value of β_c. The dip is quite broad, however, and doesn't pinpoint β_c; the distinction between the $\beta = .218$ and .210 points in the figure may be a statistical artifact. For $N = 4096$, for instance, with better statistics we find that the mean size is measured to be $571.8 \pm 1.9, 571.1 \pm 1.9, 573.1 \pm 1.9, 572.0 \pm 1.8$ and 572.6 ± 1.9 for $\beta = .211, .213, .215, .216273$ and the .218. Thus we observe no significant variation over a range $\delta\beta = .007$. On

[5] More detail on critical slowing down for various algorithms applied to spin models on random lattices will appear in future work [26].

[6] Note that this does not equal the susceptibility χ_N defined in section (2). χ_N contains no subtractions and agrees with the continuum susceptibility only in the high-temperature phase.

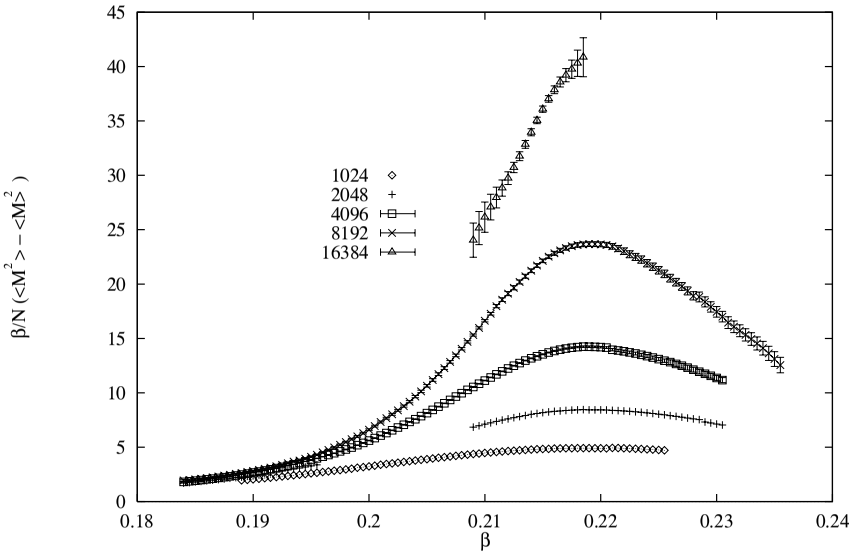

Figure 1: The 'lattice susceptibility' plotted for the one-species model for lattices of size $1024 - 16384$. Error bars are only shown when they are larger than the symbols.

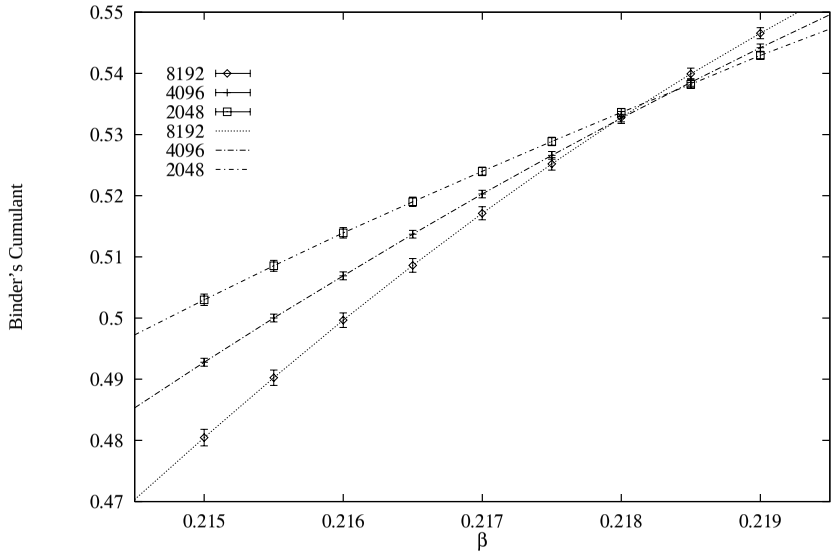

Figure 2: Binder's cumulants $\mathcal{U}_M$ for $N = 2048, 4096$ and 8192 lattices in simulations of the one species Ising model for lattices of size $1024 - 16384$. Lines are drawn to guide the eye.

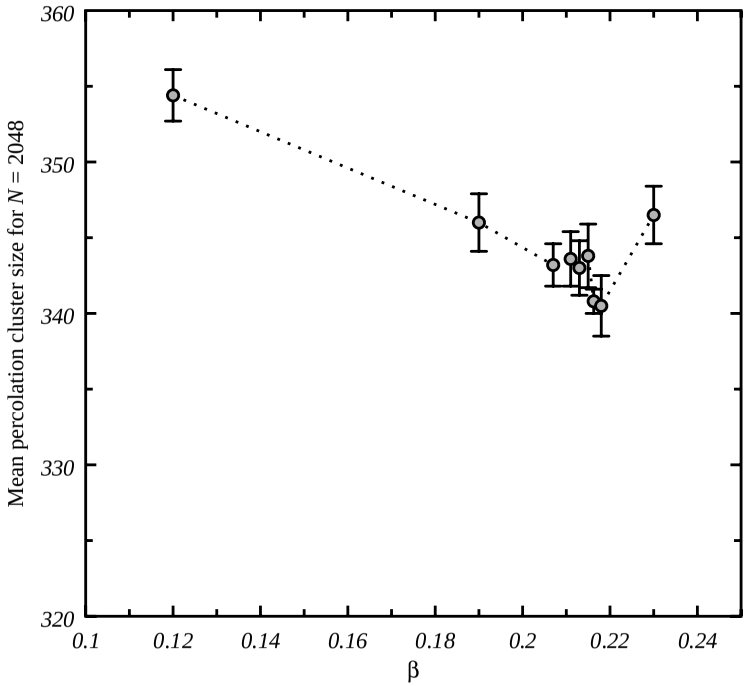

Figure 3: The mean size of percolation clusters as a function of β for the one species Ising model on 2048 node lattices. The dip occurs near criticality. The dotted line is drawn to guide the eye.

N	1024	2048	4096	8192	theory
$(\gamma/\nu d_H)_{eff}$ from χ	.702 (6)	.705 (5)	.686 (6)	.688 (10)	2/3
$(\gamma/\nu d_H)_{eff}$ from $\mathcal{S}_{FK}$		.701 (7)	.690 (9)	.676 (12)	2/3
$(d_f/d_H)_{eff}$		.844 (5)	.839 (7)	.830 (8)	5/6
$(\gamma/\nu d)^{eff}_{q=1}$		.747 (6)	.741 (7)	.722 (10)	.710
$(d_f/d_H)^{eff}_{q=1}$		.866 (5)	.866 (6)	.852 (8)	.855

Table 1: Summary of exponents extracted from finite-size scaling at the exact value of β_c for one Ising species. The exponents are computed using data from lattices of size N and $2N$.

the other hand the breadth of the dip means that measurements of $(\gamma/\nu d_H)_{q=1}$ are not very sensitive to the estimated value of β_c. This is not true for the exponent $(\gamma/\nu d_H)$ which, as we shall see, exhibits a strong dependence on the estimated critical temperature.

From the finite-size scaling relation (10) we define the effective exponents

$$(\gamma/\nu d_H)_{eff} \equiv \ln\left(\frac{\chi_{2N}}{\chi_N}\right) / \ln 2. \tag{25}$$

When cluster sizes rather than the spin–susceptibility are considered, it is implicit that $\mathcal{S}$ is to be substituted for χ in the above definition. Likewise,

$$(d_f/d_H)_{eff} \equiv \ln\left(\frac{\mathcal{M}_{2N}}{\mathcal{M}_N}\right) / \ln 2. \tag{26}$$

As usual, the analogous exponents for pure percolation are defined as above with subscript $q = 1$. We now summarize our results for these critical exponents, extracted through finite size scaling of χ_N, the mean FK cluster size $\mathcal{S}_{FK}$, the maximal FK cluster size $\mathcal{M}_{FK}$, the mean percolation cluster size $\mathcal{S}_{q=1}$ and the maximal percolation cluster size $\mathcal{M}_{q=1}$. In table (1), we present these values obtained from runs at the known value of $\beta_c \sim .216273$. The exact values are $\gamma/\nu d_H = 2/3$, $d_f/d_H = 5/6$, $(\gamma/\nu d_H)_{q=1} = (4 - \sqrt{7/2})/3$ and $(d_f/d_H)_{q=1} = (7 - \sqrt{7/2})/6$. The agreement between our measurements and the theoretical predictions is quite good. Since (d_f/d_H) only describes properties of the largest cluster, it might be less subject to corrections to scaling (for small cluster sizes) and thus provide the best estimator of the critical exponents. Indeed, the values of $(d_f/d_H)_{eff}$ for FK and percolation clusters on the larger lattices already match the asymptotic predictions, within our statistics. The exponents $(\gamma/\nu d_H)_{eff}$ decrease towards their asymptotic values and differ from them by only about 2% on the largest lattices.

N	1024	2048	4096	8192	theory
$(\gamma/\nu d_H)_{eff}$ from χ	.74 (3)	.76 (3)	.73 (2)	.76 (4)	2/3
$(\gamma/\nu d_H)_{eff}$ from $\mathcal{S}_{FK}$		.748 (14)	.741 (8)		2/3
$(d_f/d_H)_{eff}$		.877 (15)	.869 (6)		5/6
$(\gamma/\nu d)_{eff,q=1}$		.750 (10)	.739 (8)		.710
$(d_f/d_H)_{eff,q=1}$		.871 (7)	.867 (5)		.855

Table 2: Summary of exponents extracted from finite-size scaling using the numerically determined value of β_c for one Ising species.

In the two species case we do not, however, know β_c. To use the single species model as a control, therefore, we estimate the critical exponents using finite-size scaling at an estimated value of $\beta_c = .2180(7)$. We present these estimates in table 2. The values quoted from the scaling of χ characterize the range of exponents in the window $\beta \in [.2173, .2187]$; this determination relies on histogramming. The exponents extracted from cluster data are taken from data at $\beta = .218$ (within this window), since histogramming was not reliable for this data. We see that the shift in temperature away from the exact β_c induces a large change in the Ising exponents. In particular, $(\gamma/\nu d_H)_{eff}$, which previously came within 2% of the asymptotic value on the largest lattice, now is 10–15% higher. The percolation exponents fare much better; they are quite insensitive to the value of β and agree with the values taken at $\beta_c = .216273$.

We also attempted to perform a direct fit of χ to $(\beta - \beta_c)^{-\gamma}$. We found that a power law fit only seemed to work in the region $\beta = .19 - .195$, where finite size effects were not severe. Only two of our data points (corresponding to the lowest values of β at which we ran) were then used in this fit, yielding $\gamma = 1.8(1)$, which is not so far from the theoretical value of $\gamma = 2$ that follows from (12). Given the sparsity of our data in this regime and thus the difficulty in verifying that we are seeing asymptotic scaling, these results should be interpreted with caution.

We now turn to a treatment of the two species results. First, we present plots of $\beta/N(\langle M^2 \rangle - \langle |M| \rangle^2)$ and the intersections of Binder's cumulants.

Note that these observables look qualitatively very similar to their one species counterparts. The position of the susceptibility peak is $\beta = .2185^{+35}_{-20}$. The Binder's cumulants (taken from the largest lattices where we have sufficient data to determine intersections) give $\beta_c = .217(1)$. As in the one-species case we adopt the Binder's estimate, which seems to be more precise. Based on the logarithmic corrections to scaling discussed in section 2, we would estimate that on the lattice sizes simulated we are further from the asymptotic scaling regime than in the one species case. It is therefore likely that our estimate of β_c here is

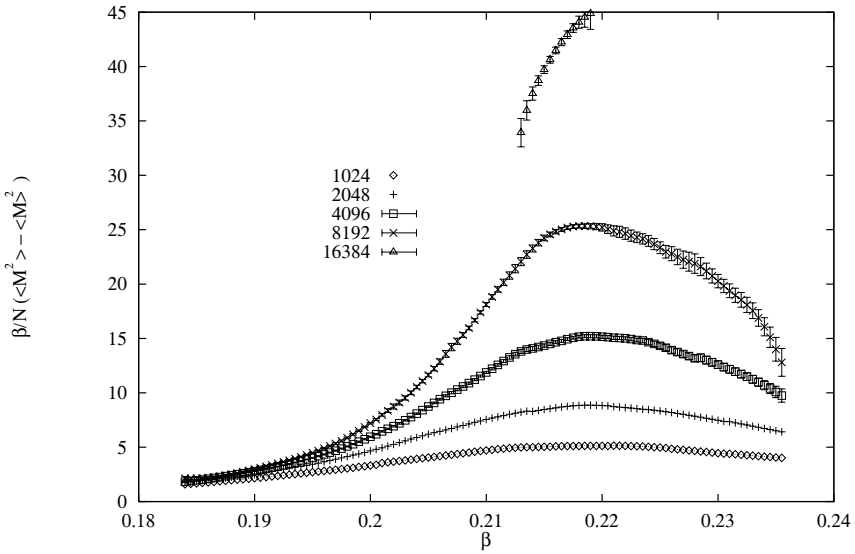

Figure 4: A plot of the 'lattice susceptibility' for the two species case with $N = 2048, 4096, 8192$ and 16384. Error bars are only shown when they are larger than the symbols.

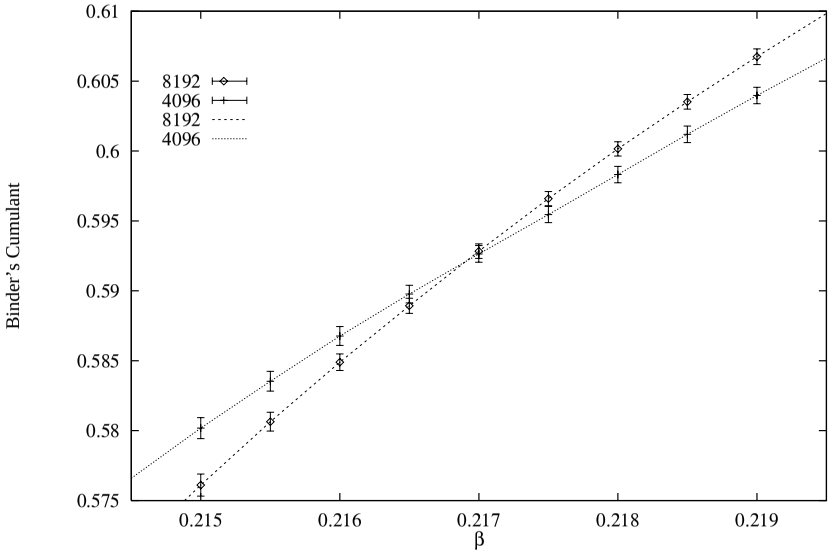

Figure 5: Binder's cumulants for $N = 4096$ and $N = 8192$ as measured in the two species model.

	1024	2048	4096	8192	theory
$(\gamma/\nu d)_{eff}$ from χ	.73 (3)	.73 (3)	.75 (5)	.74 (4)	1/2
$(\gamma/\nu d)_{eff,q=1}$	.759 (11)	.717 (5)	.712 (7)	.709 (10)	.544
$(d_f/d_H)_{eff,q=1}$	.852 (6)	.848 (4)	.848 (5)	.848 (6)	.772
$(\gamma/\nu d)_{eff,q=1}(X)$	.739 (7)	.732 (7)	.700 (10)		.544
$(d_f/d_H)_{eff,q=1}(X)$	.861 (5)	.859 (7)	.841 (8)		.772

Table 3: Summary of exponents extracted from finite-size scaling for two Ising species compared with KPZ exponents, without logarithmic corrections. In the last two rows, we present the corresponding percolation exponents for lattices on which a Gaussian field X was simulated.

less precise.

In table 3, we compare the finite-size scaling measurements of $(\gamma/\nu d_H)_{eff}$ and $(\gamma/\nu d_H)^{eff}_{q=1}$ with the theoretical exponents, computed from the KPZ formula, neglecting logarithmic corrections. The first row contains an estimate of the susceptibility exponent based on histogram extrapolations within the region $\beta = .216$ to $.218$. We observed that measuring the mean-size of FK clusters (at $\beta = .216$) always yielded exponents agreeing with those extracted from the spin–susceptibility. Since the cluster data did not histogram reliably, it was difficult though to estimate the corresponding exponents throughout the above range of β without taking a large amount of additional data. FK cluster scaling was primarily measured just to verify that it agreed with the scaling of the spin–susceptibility. Our data already showed this, so it did not seem worthwhile to repeat runs to measure the cluster scaling at various temperatures. The following rows thus summarize data for pure percolation clusters, which was relatively insensitive to β; i.e. a shift of β of .005 did not induce a stastically significant change in the $q = 1$ exponents. Since again percolation cluster data did not histogram reliably, we present data taken at $\beta = .216$ in table 3; these should be representative of the values one would measure throughout the region $\beta \in [.216, .218]$. The final two rows include exponents extracted from simulations of a Gaussian field X coupled to gravity, as discussed in [14].

What is most striking about the measured $c = 1$ exponents is in fact that they agree quite well with the $c = 1/2$ data (taken from the numerically estimated range of β_c) and in the case of percolation, the $c = 1/2$ theoretical predictions. There is clearly, however, a very large discrepancy between the measured and theoretical $c = 1$ scaling exponents. On the larger lattices, the percolation exponents for the two species Ising model also agree fairly well with those measured in the Gaussian field simulations, suggesting some degree of universality at $c = 1$ in their behavior. From equations (21) and (22), we can determine the

logarithmic corrections to the exponents $(\gamma/\nu d_H)_{eff}$ and $(\gamma/\nu d_H)^{eff}_{q=1}$. One can easily see that these are considerable by including the leading correction, which gives

$$(\gamma/\nu d_H)_{eff} = \gamma/\nu d_H + \frac{1+\gamma/\nu d_H}{\ln N} + \cdots; \tag{27}$$

this formula of course holds for $q = 1$. In Fig. 6 we compare the measured $(\gamma/\nu d_H)_{eff}$ with the corresponding theoretical predictions including both the leading correction (27) and all of the logarithmic corrections that follow from equations (21) and (22). The data does not agree particularly well with any of the predictions, but that is to be expected, since our estimate of β_c most likely induces a large error. Note that the theoretical curve including logs lies very close to the $c = 1/2$ asymptotic value of $\gamma/\nu d_H = 2/3$ for the lattice sizes we simulate. The measured values of this exponent for $c = 1$ and $c = 1/2$ (when we use the numerically estimated values of β_c) are essentially identical, so that the discrepancy between the theoretical predictions (incorporating logs in the $c = 1$ case) and the data are thus roughly the same for $c = 1$ and $c = 1/2$.

In Fig. 7 a similar comparison is shown for the exponent $(\gamma/\nu d_H)^{eff}_{q=1}$. We see that the data and theoretical predictions match quite well. Presumably, as in the $c = 1/2$ case, the comparison works because this exponent no longer depends sensitively on our determination of β_c. The agreement with theory is about as successful as in the Gaussian case [14]. This suggests the likelihood that at least the leading logarithmic corrections to scaling (27) are correct and universal for $c = 1$. We should note here that although the data can be fit by including the above logarithmic corrections it would not be possible to extract these corrections from the data itself without theoretical guidance.

As in the one species case, we also fitted our lowest β data points to $\chi \sim (\beta - \beta_c)^{-\gamma}$. The fit yielded $\gamma = 2.03(4)$ which does not match the theoretical value of $\gamma = 1 + 1/\sqrt{2} \sim 1.71$. It is not clear that this fit is reliable; probably the exact relation between χ and β should also include logarithmic corrections.

We finally turn to an examination of correlations (defined in (24) and (23)) between the different spin species. Fig. 8 exhibits definite, though moderately small, correlations between the spins of different species. As evident in Fig. 9, the correlations between the average species' energies, as measured by e^*, are much smaller. The magnetization (and more directly, the susceptibility) is strongly correlated with the distribution of FK cluster sizes, which in turn should be sensitive to the bottlenecks which characterize the worldsheet geometry. Since the correlations between species are mediated by fluctuations in the geometry, it is not surprising that they are stronger in the magnetic sector than in the energy sector. In both cases the correlations are not so strong, indicating that the Ising spins are only weakly coupling to gravity for the lattice sizes we consider.

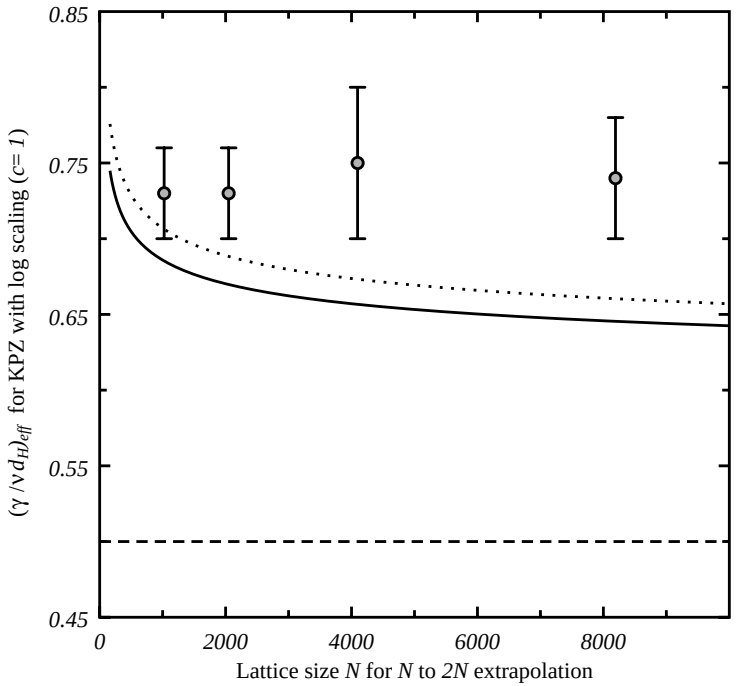

Figure 6: A comparison of the theoretical prediction of the finite–size $c = 1$ magnetic susceptibility scaling with our data. The dotted line includes the leading logarithmic correction and the solid line takes into account all subleading terms that we calculated. The horizontal dashed line represents the prediction without logarithmic corrections.

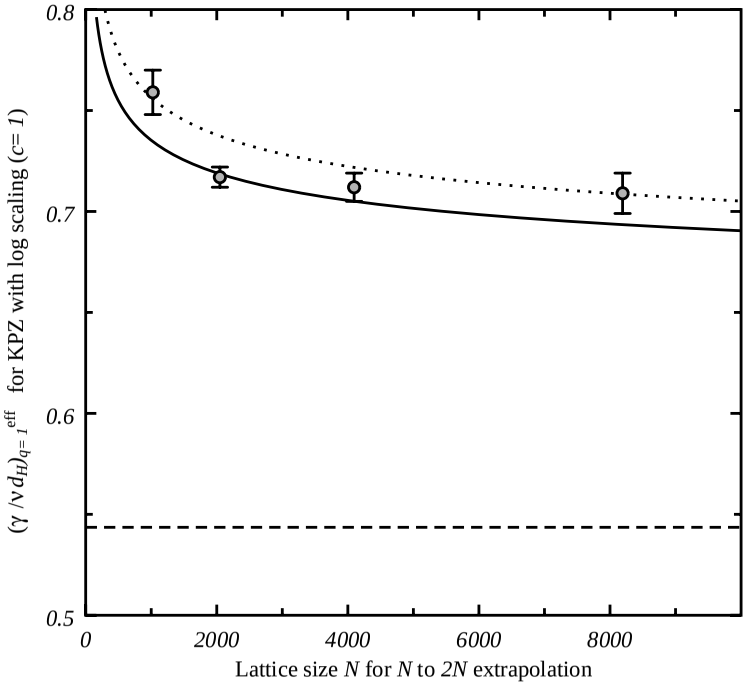

Figure 7: A comparison of the theoretical prediction of the finite size $c = 1$ scaling of $(\gamma/\nu d_H)_{q=1}$ with our percolation data for the two species Ising model. The dotted line includes the leading logarithmic correction and the solid line takes into account all subleading terms that we calculated. The horizontal dashed line indicates where these curves asymptote.

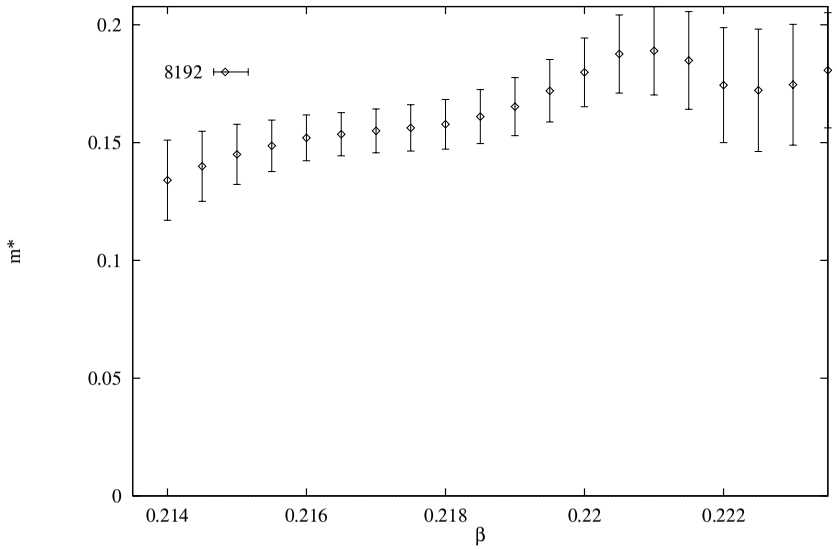

Figure 8: The correlation m^* plotted for the two species model on $N = 8192$ lattices. Recall that the correlations are normalized so that m^* equals one when $|M^{\alpha=1}|$ and $|M^{\alpha=2}|$ are fully correlated.

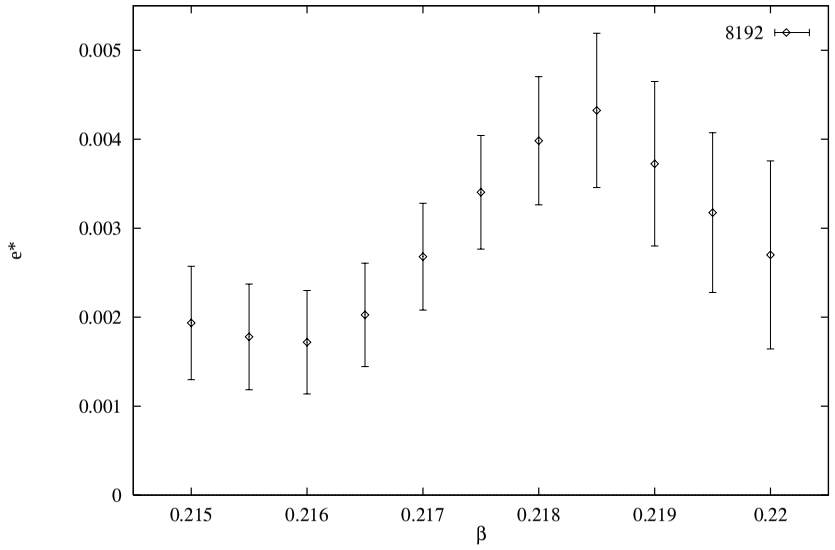

Figure 9: The correlation e^* between the energies of different species plotted for the $c = 1$ model on $N = 8192$ lattices.

4 Discussion

To gauge our prospects for extending this work to $c > 1$, we shall now attempt to shed more light on the origin of the corrections to scaling at $c = 1$. The dynamics at $c = 1$ is governed by the tachyon (the lowest mass operator) which acquires a continuous spectrum with vanishing energy at 0 momentum. The scaling corrections arise from the infrared cutoff on the tachyonic momentum, $p > 1/\ln N$ [13]. The origin of this logarithmic cutoff may not be so evident in the context of the two-species Ising model, since the tachyon cannot be expressed so simply in terms of the Ising spins. The presence of logarithmic corrections appears to only depend on the value of the central charge, so we appeal to universality and consider instead the $c = 1$ Gaussian theory. The tachyon can then be written in terms of the Gaussian field X as

$$T(p) \sim \int \sqrt{|\hat{g}|} \exp(ipX + (|p| - 2)\phi); \tag{28}$$

ϕ is the Liouville field and $\hat{g}$ is the reference metric ($g = \hat{g} \exp(-\phi)$). The infrared target space momentum cutoff is then just a consequence of the infinite Hausdorff dimension of the embedding space [30],

$$\langle XX \rangle \sim (\ln N)^2. \tag{29}$$

The suppression of tachyon propagation by finite-size effects effectively weakens the coupling between gravity and the Ising spins. Therefore, the spins of each species are only very weakly coupled, and the two and one species models appear to be qualitatively very similar on the lattices we consider. This should not be true in the continuum limit. We see that without an understanding of the corrections to scaling for $c = 1$, the numerical observations seem to conflict with our theoretical expectations of the onset of strong coupling at $c = 1$.

The target space Hausdorff dimension, as measured for Gaussian embeddings of d somewhat greater than 1, is also large. Thus we would expect that for $c > 1$, the tachyon ground state energy still acquires a considerable shift and we expect large corrections to scaling. At $c = 1$, we were able to determine these corrections because the $c = 1$ model is solvable. Without new theoretical input, the prognosis for understanding simulations for c somewhat greater than 1 thus seems poor.

5 Acknowledgments

This work has been done with NPAC (Northeast Parallel Architectures Center) computing facilities. We would like to thank John Apostolakis, Simon Catterall and Paul Coddington for helpful correspondence and conversations. The research of MB was supported by the Department of Energy Outstanding Junior Investigator Grant DOE DE-FG02-85ER40231, that of MF by funds from NPAC and that of GH by research funds from Syracuse University.

References

[1] P. Di Francesco, P. Ginsparg and J. Zinn-Justin, 2D Gravity and Random Matrices, hep-th/9306153, to appear in Phys. Rep.

[2] V. G. Knizhnik, A. M. Polyakov and A. B. Zamolodchikov, Mod. Phys. Lett. **A3** (1988) 819.

[3] D. Kutasov and N. Seiberg, Nucl. Phys. **B358** (1991) 600.

[4] G. Moore and P. Ginsparg, Lectures on 2-D Gravity and 2-D String Theory, TASI Lectures, Yale preprint YCTP-P23-92 and Los Alamos preprint LA-UR-92-3479 (1993), hep-th/9304011.

[5] V. A. Kazakov, Phys. Lett. **A119** (1986) 140.

[6] D. V. Boulatov and V. A. Kazakov, Phys. Lett. **B186** (1987) 379.

[7] E. Brézin and S. Hikami, Phys. Lett. **B283** (1992) 203.

[8] S. Hikami and E. Brézin, Phys. Lett. **B295** (1992) 209.

[9] S. Hikami, Phys. Lett. **B305** (1993) 327.

[10] C. Baillie and D. Johnston, Mod. Phys. Lett. **A7** (1992) 1519; Phys. Lett. **B286** (1992) 44.

[11] S. M. Catterall, J. B. Kogut and R. L. Renken, Phys. Rev. **D45** (1992) 2957; Phys. Lett. **B292** (1992) 277.

[12] J. Ambjørn, B. Durhuus, T. Jónsson and G. Thorleifsson, Nucl. Phys. **B398** (1993) 568.

[13] I. Klebanov, String Theory in Two-Dimensions, in Proc. of the Trieste School on String Theory and Quantum Gravity '91 (hep-th/9108019).

[14] Geoffrey Harris, Percolation on Strings and the Cover-up of the c=1 Disaster, Syracuse University preprint SU-HEP 4241-555.

[15] F. David, Mod. Phys. Lett. **A3** (1988) 1651; J. Distler and H. Kawai, Nucl. Phys. **B321** (1989) 509.

[16] C. M. Fortuin and P. W. Kasteleyn, Physica **57** (1972) 536.

[17] A. Sokal, Monte Carlo Methods in Statistical Mechanics: Foundations and Algorithms, NYU preprint based on lectures at the Troisième Cycle de la Physique en Suisse Romande, June 1989.

[18] C.-K. Hu, Phys. Rev. **B29** (1984) 5103.

[19] D. Stauffer and A. Aharony, Introduction to Percolation Theory (Taylor and Francis, London, U.K. 1992).

[20] M. den Nijs, Phys. Rev. **B27** (1983) 1674.

[21] M. F. Sykes and J. W. Essam, J. Math. Phys. **5** (1964) 1117.

[22] P. Ginsparg, in Fields, Strings and Critical Phenomena, Les Houches Proceedings, Vol. 49, ed. E. Brézin and J. Zinn-Justin (North Holland, Amsterdam 1983) 5.

[23] J. Ambjørn, D. Boulatov and V. A. Kazakov, Mod. Phys. Lett. **A5** (1990) 771.

[24] D. Boulatov, V. Kazakov, I. Kostov and A. A. Migdal, Phys. Lett. **B157** (1985) 295.

[25] R.H. Swendsen and J.-S. Wang, Phys. Rev. Lett. **58** (1987) 86.

[26] M. Bowick, M. Falcioni, G. Harris and E. Marinari, to appear.

[27] M. Falcioni, E. Marinari, M. L. Paciello, G. Parisi and B. Taglienti, Phys. Lett. **102B** (1981) 270; A. M. Ferrenberg and R. H. Swendsen, Phys. Rev. Lett. **61** (1988) 2635; and *Erratum*, ibidem **63** (1989) 1658.

[28] K. Binder, Z. Phys. **B43** (1981) 119.

[29] Z. Burda and J. Jurkiewicz, Acta Physica Polonica **B20** (1989) 949.

[30] V. A. Kazakov and A. A. Migdal, Nucl. Phys. **B311** (1988) 171.